

Multi-spin exchange model the near melting transition of the 2D Wigner crystal

B. Bernu[†] and D. M. Ceperley[‡]

[†] Laboratoire de Physique Thorique des Liquides, UMR 7600 of CNRS, Universit P. et M. Curie, boite 121, 4 Place Jussieu, 75252 Paris, France,

E-mail: bernu@lptl.jussieu.fr

[‡] Dept. of Physics and NCSA, University of Illinois, Urbana-Champaign, Urbana, IL 61801, USA

E-mail: ceperley@uiuc.edu

Abstract. The low temperature properties of fermionic solids are governed by spin exchanges. Near the melting transition, the spin-exchange energy increases as well as the relative contribution of large loops. In this paper, we check the convergence of the multi-spin exchange model and the validity of the Thouless theory near the melting of the Wigner crystal in two dimensions. Exchange energies are computed using Path Integral Monte Carlo for loop sizes up to 8, at $r_s = 40, 50$ and 75 . The data are then fitted to a geometric model. Then the exchange energies are extrapolated to larger sizes in order to evaluate their contributions to the leading term of the magnetic susceptibility and the specific heat. These results are used to check the convergence of the multi-spin exchange model.

1. Introduction

^3He atoms as well as electrons carry a spin $1/2$. In their solid phases, exchange processes are responsible for the thermodynamics at low temperature. The Thouless theory explains how a Multi Spin Exchange (MSE) effective Hamiltonian results from these spin exchanges[1]. The applicability of such an approach is based on the very different scales of the exchange energies and the phonon energies (at least 3 orders of magnitude). In the strong coupling limit ($r_s \rightarrow \infty$ for the Wigner crystal), a semiclassical calculation (WKB) predicts such very small exchange energies. Moreover, in this limit, only the two or three body exchanges dominate depending on the dimension and the lattice type, leading to the standard Heisenberg model (for spin $1/2$, three body exchanges are equivalent to pair exchanges). Then, at weaker coupling, other loop exchanges arise that may lead to a magnetic phase transition. In general, more and more exchanges are important near the melting transition. The problem we address here is how the MSE Hamiltonian evolves as we approach the melting transition and whether there is a precursor to melting in the magnetic Hamiltonian.

Exchange energies have been obtained for the bulk 3D ^3He [3] and for ^3He adsorbed on graphite[4]. The exchange energies have been obtained as well for the 2D electron Wigner crystal[5]-[6]. For most densities, from the semiclassical limit to near melting, the WKB and Path Integral Monte Carlo (PIMC) evaluations assume a stable solid of particles (a triangular lattice in 2D) without taking into account the Fermi

statistics. For these densities, only small exchange loops with 6 or fewer particles have significant energies. These calculations determine the exponential dependence of exchange energies versus the density; the longer loops decreasing more rapidly in the strong coupling limit. The MSE model explains the main features of the magnetic transition of the second solid layer of helium 3 adsorbed on graphite[7].

One problem that has been encountered near melting is that the PIMC calculations become increasingly difficult to converge. This is because the Boltzmann solid melts before the fermion solid. Adding Fermi statistics stabilizes the solid in a wider density region. (Or alternatively, imposing antisymmetry increases the energy of the liquid phase into which the crystal melts.) In order to stabilize the crystal, we assume a ferromagnetic spin polarization of “spectator” atoms (non-exchanging atoms) and enforce antisymmetry on those paths. When comparison is possible, only small changes of exchange energies are found with this procedure. The largest differences are seen at $r_s = 50$ for the system without statistics where the solid is close to melting (melting of the bosonic wigner crystal occurs at $r_s \approx 60$). The restriction on the path resulting from Fermi statistics does not modify the exchange energies very much. The statistics do not affect the local correlated motions of particles in the vicinity of the exchanging ones. But statistics have long range effects that stabilize the solid and forestall the melting.

The next question is whether the Thouless theory can be applied near the melting transition. Indeed, a possible scenario could be that the energy difference associated with a given spin-exchange, say J_P , becomes comparable to the zero-point motion kinetic energy ($k_e^{(0)}$). In that case, a complicated coupling between spin states and phonon excitations could arise. Instead our numerical results demonstrate, that all the exchange energies are much smaller than $k_e^{(0)}$ even at melting. Even if the exchange energy increases exponentially with the inverse density (WKB predicts $-\log(J) \propto r_s^{1/2}$), each value stays well below $k_e^{(0)}$. Thus, up to the melting transition, each exchange can be seen as an independent event.

Now, near the melting transition, the number of *important* exchanges increases considerably. In this paper, we address the question of the convergence of this MSE model versus the number of exchanges. Indeed, if the exchange energies decrease roughly exponentially with the loop size n , the number of loops of size n does increase exponentially. The convergence of the MSE model is thus questionable. Does the total spin-exchange energy diverge when the crystal melts? Is the existence of long-exchanges a mechanism for the melting transition or a by-product? We try to answer these questions from the analysis of the two-dimensional Wigner crystal exchange data. In section II, we present the results of Path Integral Monte Carlo (PIMC) simulations and we give the formula to test the convergence of the MSE model. In section III, different models are used to fit PIMC results in order to extrapolate to larger loop sizes.

2. PIMC Results and Thermodynamics

For a given permutation P , the exchange energy J_P calculated from PIMC needs to be monitored carefully with respect to several parameters such as the number of particles and the time step τ . There are additional parameters associated with the Bennett method. Fortunately, those parameters change smoothly with the density or the type of exchange or even the system (Helium atoms or electrons). The most important

effect is the $\beta = 1/T$ dependence of the results. Indeed, the calculations are done at a temperature sufficiently low so that the phonon excitations are non-existent but sufficiently high that the spins have not magnetically ordered. In these conditions, the exchange energy should be independent of the temperature. However, near melting (the precise density depends on the statistics) results show a linear increase versus β (note that each independent run at a given temperature is well converged). This is in fact interpreted as a signature of melting that would most probably occur for larger systems. The following tables contain only exchange values converged and independent of β .

Table 1 shows the PIMC results. Shown are the energies versus exchange for the 3 densities considered. It is seen that exchange energies decrease as r_s increase or at fixed r_s , when the loop size increases. The strong dependence on the shape of the exchange we examine next.

The overall importance of the exchange processes can be measured by the leading term of the high temperature (HT) expansion of the magnetic susceptibility (the Curie-Weiss temperature θ) and the specific heat:

$$\theta = - \sum_{n=2}^{n_{\max}} (-1)^n \frac{n(n-1)}{2^{n-1}} J_n^{(T)} \quad (1)$$

where

$$J_n^{(T)} = \sum_{\text{shape of } n \text{ sites}} n_{\text{shape}} J_n^{(\text{shape})} \quad (2)$$

with n_{shape} is the number of loops per site of a given *shape* and $J_n^{(\text{shape})}$ the associated exchange value.

The leading HT-term of the specific heat is defined as

$$\lim_{T \rightarrow \infty} \frac{C_V(T)}{Nk_B} \sim \frac{9}{4} \left(\frac{J_{C_V}}{T} \right)^2 \quad (3)$$

where J_{C_V} is given by a positive quadratic form of the exchange values:

$$J_{C_V}^2 = \sum_{ij} J_i M_{ij} J_j. \quad (4)$$

Unfortunately, no simple formula exists for the matrix M . At very large r_s (WKB limit) only J_2 and mainly J_3 dominate in a ferromagnetic phase and $|\theta| = J_{C_V} = J_2 - 2J_3$. At $r_s \sim 200$, J_4 is large enough and the system becomes anti ferromagnetic.

3. Fits of exchange energies to analytic formula

In order to determine the contribution of larger exchanges to the magnetic susceptibility and specific heat in Eqs.1,3, we want to understand how exchange energies vary with the loop size and shape.

Exchange energies depend mainly on the loop size n . Then, for a given loop size n , the exchange is much larger if the exchange contains only smooth angles, that is when its area \mathcal{A} is maximum ($\mathcal{A} = (n-2+2p)\mathcal{A}_0$, where \mathcal{A}_0 is the area of the enclosed triangles and p is the number of lattice sites inside the loop). In order to quantify this shape dependence we assume that each local section of the exchange contributes to the exchange probability and use the following formula:

$$\log(J_{n,s}^{fit}) = \alpha_0 + \alpha_n n + \alpha_p p_s + \sum_v \alpha_v N_{s,v}. \quad (5)$$

J	mult	$r_s=40$		$r_s=50$		$r_s=75$	
2	3	1402.	2%	323.	3%	13.4	3%
3	4	1184.	3%	281.	3%	14.2	2%
4	6	809.	3%	165.	5%	6.2	3%
5	12	295.	6%	42.	7%	1.1	6%
6 ₁	2	476.	5%	88.	9%	2.3	11%
6 ₂	12	143.	7%	17.1	8%	0.24	8%
6 ₃	12	92.	8%	9.	9%	0.116	9%
6 ₄	4	40.	13%	3.2	8%	0.021	8%
7 ₁	12	105.	9%	14.4	6%	0.16	18%
7 ₂	12	72.	11%	7.8	9%	0.076	21%
7 ₃	24	43.	11%	3.6	9%	0.018	13%
7 ₄	12	37.	21%	2.8	16%	0.0037	19%
7 ₅	24	20.	15%	0.97	11%	0.004	17%
8 ₁	6	130.	11%	15.3	7%		
8 ₂	6	29.	13%	1.74	9%		
8 ₃	12	19.	12%	1.19	10%		
8 ₄	12	23.	10%	1.72	7%		
8 ₅	24	40.	13%	3.1	9%		
8 ₆	12	44.	12%	3.5	11%		
8 ₇	6	1.3	21%	0.058	17%		
8 ₈	12	4.3	26%	0.32	26%		
8 ₉	24	6.4	24%	0.25	21%		
8 ₁₀	12	23.	11%	1.5	14%		
8 ₁₁	24	7.6	14%	0.25	20%		
8 ₁₂	24	18.	18%	0.97	11%		
8 ₁₃	12	8.8	16%	0.24	15%		
8 ₁₄	24	22.	10%	2.5	8%		
8 ₁₅	24	9.8	14%	0.51	10%		
8 ₁₆	12	14.	12%	1.08	8%		
9 ₁	4	75.	15%	5.2	10%		

Table 1. Exchanges energies (in $10^{-9} Ry$) obtained by PIMC simulations for the fully polarized 2D Wigner crystal. Results are for 64 electrons, and respectively $\beta = 1/T = 10000, 16600, 20000 Ry^{-1}$, time step $\tau = 40, 66, 100 Ry^{-1}$ for $r_s = 40, 50, 75$. The multiplicity is the number permutation P of the same shape per site, including P^{-1} symmetry. All exchanges are for nearest neighbor on the triangular lattice. For 2 through 6 particle exchange there is only one sort of diagram, but for larger exchanges there are multiple possibilities which we have labelled arbitrarily with an index. The authors can be contacted for further details.

Here p_s is the number of non-exchanging sites contained inside the loop of shape s and $N_{s,v}$ is the number of patterns of type v encountered in the loop of shape s . The α 's are parameters determined from a least-squares fit minimizing:

$$\chi^2 = \frac{1}{N_J} \sum_{n,s} \left(\frac{\log(J_{n,s}/J_{n,s}^{fit})}{\sigma_{n,s}} \right)^2, \quad (6)$$

where N_J are the number of degrees of freedom (the number of exchanges minus the number of fitting parameters), and $\sigma_{n,s}$ is the Monte Carlo error of $\log(J_{n,s})$. We now

r_s	40	50	75
α_0	8.99(4)	8.34(5)	6.79(6)
α_p	0.91(3)	1.09(3)	2.52(1)
α_n	-0.752(9)	-1.038(9)	-1.466(14)
χ	8.5	9.5	16.0

r_s	40		50		75	
α_0	12.1(1)		12.32(1)		12.9(2)	
α_p	0.19(4)		0.14(4)		0.39(12)	
α_{v_0}	-0.883(14)		-1.185(12)		-1.954(2)	
$\alpha_{v_{60}}$	-1.009(14)	1.14	-1.28(12)	1.08	-2.05(3)	1.04
$\alpha_{v_{120}}$	-1.69(3)	1.91	-2.28(3)	1.92	-3.43(7)	1.75
χ	2.5		4.5		5.0	

r_s	40		50	
α_0	11.3(7)		8.8(5)	
α_p	0.03(8)		-0.07(7)	
α_{w_0}	-0.63(5)		-0.8(4)	
α_{w_1}	-0.76(4)	1.20	-0.8(4)	1.0
α_{w_2}	-1.27(11)	2.01	-1.25(9)	1.56
α_{w_3}	-0.93(4)	1.47	-1.15(3)	1.43
α_{w_4}	-0.87(1)	1.38	-0.69(8)	0.86
α_{w_5}	-1.37(6)	2.17	-1.65(5)	2.06
α_{w_6}	-1.15(16)	1.82	-0.92(13)	1.15
α_{w_7}	-1.44(7)	2.28	-1.94(5)	2.42
χ	1.3		1.3	

Table 2. Top Table : Fit of exchange energies according to Eqs. 5-6. α_n is the main varying parameter. Uncertainties are in parenthesis. Middle Table : Same for fits with the 2 links patterns. For each r_s , the third column is the ratio v_i/v_0 : within error bars, they are independent of r_s for this model. Bottom Table : same for 3 links patterns. For each r_s , the third column is the ratio w_i/w_0 , the ratio depends on r_s for patterns with smooth angles, and not for patterns with sharp angles.

discuss the results for the fit allowing for 3 successively more detailed patterns.

Fitting without patterns. Without using any of the parameters that depend on the shape of the exchange ($\alpha_v = 0$), only 3 parameters remain: α_0 , α_n and α_p . The results are given in table 2-Top. Such a fit is not accurate as can be seen by the large value of χ^2 . As an interpretation of the parameters, $\exp(\alpha_0)$ is the prefactor for the initiation of an exchange, α_n is the action needed for adding a link onto the exchange, and α_p , is a term which favors non-compact exchanges.

Fitting with 2-links patterns. The simplest patterns v consist of the angles subtended by 2 adjacent links. On a triangular lattice there are three possible cases, since two adjacent links can have angles of 0, 60, 120 or 180 degrees (see Fig.1) but the parameter v_{180} only occurs in J_2 . Also α_n is becomes redundant because it can be determined from the angles: $\sum_v N_{s,v} = n$, the number of angles equals the number of sites in the loop. Thus we are left with five parameters. The results for this fit are shown in table 2-Middle.

The mean error is significantly reduced by including the angles in the fit. We

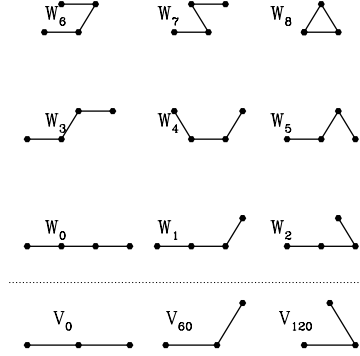


Figure 1. List of the three possible patterns made of two links (last line) and the eight patterns made of three links.

find that α_0 depends weakly on density, α_p is not very significant. Note that the ratio v_i/v_0 is almost independent of r_s .

Fitting 3-links patterns. In our most elaborate fit, the possible configurations of three adjacent link are used (see Fig. 1). The triangular pattern w_8 occurs only in the 3-body loop, thus is removed from the fitting procedure. Note that if the patterns for 3-links are used, those of 2-links are redundant. Here again α_n is a redundant parameter. Hence, we are left with 10 parameters for 28 exchanges for which we have computed exchange frequencies. At $r_s = 75$, we have not computed enough different exchanges, to do this fit so we only discuss it at smaller values of r_s .

The results are shown in Table 2-Bottom. This fit is now reasonable as the mean standard deviation is of order of one, i.e. within statistical error bars of the PIMC results. Clearly the parameter α_p can be removed. In this fit, the ratios w_i/w_0 depend on r_s except for w_3, w_5, w_7 .

4. Expanding to larger loop cycles

From the fits of the previous section, it is now possible to evaluate, at high temperature, the leading term θ of the magnetic susceptibility (see Eq.1) and J_{C_V} of the specific heat (see Eq.3) by including much larger loops. Those terms give an estimate of the temperature of the spins begin to become correlated (note that the expected ground state is a spin liquid). We test here if the MSE model still converges when more and more exchanges are involved as it appears near the melting transition.

We have calculated all self avoiding walks of length up to size $n = 22$ on the triangular lattice, with their shape properties (p , angles v and w).

Fig.2-left shows the sum J_n^T of all energies of loops of size n . J_n^T decreases at large r_s , but clearly increases exponentially at $r_s = 40$. Nevertheless the Curie-Weiss temperature seems to converge at all densities (Fig.2-Middle) even if strong oscillations appear at the $r_s = 40$.

The leading term of the specific heat J_{C_V} (Eq.3) can be used to scale energies/temperatures. A divergence of this term means a huge energy associated with

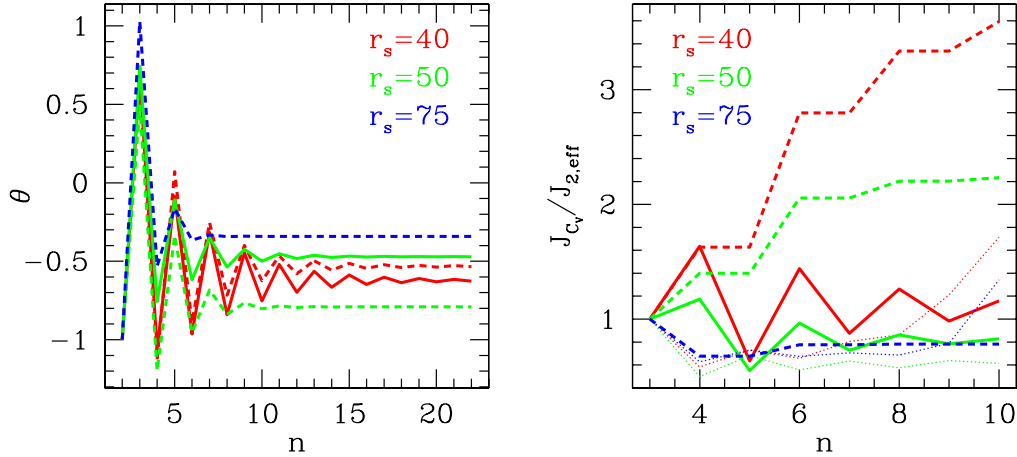


Figure 2. Left : Total Exchange energy of loops of length n versus n (see Eq.2). Middle : Contribution of loops of length n to the Curie-Weiss temperature versus n (see Eq.1). Right: Contribution of loops of length n to J_{C_V} versus n (see Eqs.3-4). The full lines stand for the model with 3-link patterns, dashed lines for the model with 2-link patterns, and the dotted line for the model without patterns (see text).

exchanges, and likely the melting of the solid. Fig.2-right shows a good convergence of J_{C_V} again at large r_s . The 2-links and 3-links models provide rather different results. This means that J_{C_V} is a rather subtle combination of exchange energies. Still all models seem to converge at $r_s = 50$. At the smallest $r_s = 40$, the 2-links model diverges, whereas the 3-links model seems to converge though with strong oscillations.

5. Conclusion

Exchange energies can be computed with Path Integral Monte Carlo up to the melting transition. Use of Fermi statistics is necessary to stabilize the solid (non-local effect), but it does not change the exchange energies (local contribution). As one approaches the melting transition, an increasing number of different exchanges becomes important. The Thouless theory allows one to write a multi-spin exchange model to describe the low energy physics. But the convergence of this model is not guaranteed and must be verified. We have checked that for the 2D Wigner crystal, the Curie-Weiss temperature θ and the first-order contribution to the specific heat ($\text{Trace}(H - \langle H \rangle)^2$) converge for the lowest densities. The large oscillations seen both these quantities at $r_s = 40$ hint at a possible divergence in the thermodynamic properties at higher densities. Though the MSE model converges at lower densities, a divergence of the model is possible at the critical melting density, consistent with the picture that multi-spin exchange is itself a mechanism for melting.

- [1] D. J. Thouless, *Proc. Phys. London* **86**, 893 (1965).
- [2] D. M. Ceperley, *Rev. Mod. Phys.* **67**, 279 (1995).
- [3] D. M. Ceperley and G. Jacucci, *Phys. Rev. Lett.* **58**, 1648 (1987).

- [4] B. Bernu and D. Ceperley in *Quantum Monte Carlo Methods in Physics and Chemistry*, eds. M.P. Nightingale and C.J. Umrigar, Kluwer (1999).
- [5] B. Bernu, L. Candido, D. Ceperley *Phys. Rev. Lett.* **86** 870 (2001).
- [6] Bernu, B., L. Candido and D. M. Ceperley Proceedings of the Rolduc school on Quantum Simulations of Complex Many Body Systems (2002). Bernu, B. and D. M. Ceperley *J. of Physics Cond. Mat.* 14, 9099 (2002), "Exchange Frequencies in 2d solids"
- [7] G. Misguich, B. Bernu, C. Lhuillier and C. Waldtmann. *Phys. Rev. Lett.* **81** 1098 (1998); *Phys. Rev. B* **60** 1064 (1999).